Atmos. Meas. Tech., 10, 3931–3946, 2017
https://doi.org/10.5194/amt-10-3931-2017

Atmospheric Measurement Techniques
Open Access
EGU

CH_4 emission estimates from an active landfill site inferred from a combined approach of CFD modelling and in situ FTIR measurements

Hannah Sonderfeld[1], Hartmut Bösch[1,2], Antoine P. R. Jeanjean[1], Stuart N. Riddick[3], Grant Allen[4], Sébastien Ars[5], Stewart Davies[6], Neil Harris[7], Neil Humpage[1], Roland Leigh[1], and Joseph Pitt[4]

[1]Earth Observation Science Group, Department of Physics and Astronomy, University of Leicester, Leicester, UK
[2]National Centre for Earth Observation, University of Leicester, Leicester, UK
[3]Department of Civil and Environmental Engineering, Princeton University, Princeton, NJ, USA
[4]Centre for Atmospheric Science, The University of Manchester, Manchester, UK
[5]Laboratoire des Sciences du Climat et de l'Environnement (LSCE/IPSL), CNRS-CEA-UVSQ, Université de Paris-Saclay, Gif-sur-Yvette, France
[6]Viridor Waste Management Limited, Peninsula House, Rydon Lane, Exeter, Devon, UK
[7]Centre for Atmospheric Informatics and Emissions Technology, Cranfield University, Cranfield, UK

Correspondence to: Hannah Sonderfeld (hs287@le.ac.uk)

Received: 23 November 2016 – Discussion started: 3 April 2017
Revised: 11 September 2017 – Accepted: 17 September 2017 – Published: 25 October 2017

Abstract. Globally, the waste sector contributes to nearly a fifth of anthropogenic methane emitted to the atmosphere and is the second largest source of methane in the UK. In recent years great improvements to reduce those emissions have been achieved by the installation of methane recovery systems at landfill sites, and subsequently methane emissions reported in national emission inventories have been reduced. Nevertheless, methane emissions of landfills remain uncertain and quantification of emission fluxes is essential to verify reported emission inventories and to monitor changes in emissions. Here we present a new approach for methane emission quantification from a complex source such as a landfill site by applying a computational fluid dynamics (CFD) model to calibrated in situ measurements of methane as part of a field campaign at a landfill site near Ipswich, UK, in August 2014. The methane distribution for different meteorological scenarios is calculated with the CFD model and compared to methane mole fractions measured by an in situ Fourier-transform infrared (FTIR) spectrometer downwind of the prevailing wind direction. Assuming emissions only from the active site, a mean daytime flux of 0.83 mg m^{-2} s^{-1}, corresponding to a spatially integrated emission of 53.3 kg h^{-1}, was estimated. The addition of a secondary source area adjacent to the active site, where some methane hotspots were observed, improved the agreement between the simulated and measured methane distribution. As a result, the flux from the active site was reduced slightly to 0.71 mg m^{-2} s^{-1} (45.6 kg h^{-1}), and at the same time an additional flux of 0.32 mg m^{-2} s^{-1} (30.4 kg h^{-1}) was found from the secondary source area. This highlights the capability of our method to distinguish between different emission areas of the landfill site, which can provide more detailed information about emission source apportionment compared to other methods deriving bulk emissions.

1 Introduction

Methane (CH_4) is the second most important anthropogenic greenhouse gas (GHG) after carbon dioxide (CO_2), with a global warming potential of 34 on a 100-year timescale (Myhre et al., 2013). Globally, the CH_4 budget is reason-

ably well known, but on local and regional scales large uncertainties remain for emissions from individual sources (Dlugokencky et al., 2011). The Climate Change Act 2008 legally binds the UK to reduce carbon emissions from GHGs by 80 % in 2050 compared to the 1990 baseline (legislation.gov.uk, 2017); therefore, a profound knowledge of CH_4 sources and their emission strength is required. The waste management sector contributed 3.7 % to the total UK greenhouse gas emissions in 2014 (Brown et al., 2016) and is the second largest source of CH_4 in the UK after agriculture (Salisbury et al., 2016).

CH_4 and CO_2 are produced during the degradation process of municipal solid waste at landfill sites. Under anaerobic conditions landfill gas (LFG) with approximately 50 % CH_4 and 45 % CO_2 is produced (Czepiel et al., 1996). The organic degradable waste is broken down in several steps by initially aerobic and eventually anaerobic bacteria. While CH_4 is formed in the final steps from acetic acid decarboxylation or reduction of CO_2, CO_2 is formed in all stages (Czepiel et al., 1996; Themelis and Ulloa, 2007) of waste degradation. Once produced there are several ways for CH_4 to be released from the landfill site. It can be released through the landfill cover, where it partially oxidises to CO_2 depending on the cover soil, or migrate underground and finally travel to the surface outside the landfill area (Scheutz et al., 2009). If a LFG recovery system is installed, the recovered CH_4 is either used for energy production or flared and thereby converted to CO_2. Modern gas recovery systems may reach efficiencies of over 90 % (Scheutz et al., 2009, and references therein).

The focus in past studies is on CH_4 emissions from closed and covered areas of landfills. Wide ranges of emissions are reported, which depend on the conditions of the site and cover. In years 1988 to 1994, Bogner et al. (1995) measured CH_4 fluxes in the range of -0.00154 to 1119 $g\,m^{-2}\,day^{-1}$ at landfill sites in the USA with different soil covers and with and without a LFG recovery system. Mønster et al. (2015) and Gonzalez-Valencia et al. (2016) report CH_4 fluxes in the range of 0.7 to 13.2 $g\,m^{-2}\,day^{-1}$ from 15 Danish landfill sites and 10 to 575 $g\,m^{-2}\,day^{-1}$ from three landfill sites in Mexico. One critical factor here is the installation and efficiency of a LFG recovery system (Bergamaschi et al., 1998).

Some studies also have analysed emissions from still-operating landfill sites. Bergamaschi et al. (1998) reports a CH_4 flux of up to 28.8 $g\,m^{-2}\,day^{-1}$ for the uncovered area of a landfill site in Germany. At most landfill sites so-called hotspots, e.g. cracks and leaks in the cover, are present, which emit much higher concentrations than the surrounding areas and have a high temporal variability (Rachor et al., 2013). To reduce uncertainty in landfill site emissions and the underrepresentation of emissions from operating areas, further accurate observations are needed.

A variety of techniques have been applied to quantify emissions from landfill sites in different stages. So far, no site-wide flux measurement approach has been fully validated, and a great effort is going into establishing the most appropriate sampling approaches and measurement technologies. As a result of their simplicity, chamber measurements are commonly used (Bogner et al., 1995; Czepiel et al., 1996; Börjesson et al., 2000; Christophersen et al., 2001; Schroth et al., 2012; Rachor et al., 2013). For this method, static or dynamic flux chambers are placed in different locations on the landfill site and are sealed to avoid air exchange with the atmosphere. The increase in concentration of the target gas inside the enclosure is monitored. The main drawback of this technique is the sparse sampling of the area covered by the chambers. Inhomogeneity in emissions over a landfill site, e.g. caused by hotspots, can give misleading results when scaling up to the whole landfill site. To overcome these difficulties a grid pattern is often chosen for placement of the chambers (Czepiel et al., 1996; Börjesson et al., 2000). Gonzalez-Valencia et al. (2016) recently tested a surface probe method for faster sampling of CH_4 emissions on discrete grid points by sampling in direct contact with the ground.

Eddy covariance (EC) systems also have been applied to measure nitrous oxide (N_2O) and CH_4 fluxes over landfill sites covering a wider area than enclosure techniques (Rinne et al., 2005; Lohila et al., 2007; Schroth et al., 2012). Although a good agreement with chamber measurements was found, this technique is dependent on the wind direction and sufficient wind speed (Lohila et al., 2007). EC systems are best suited for flat terrain and have difficulties with complex topography.

Sensors on mobile platforms offer the advantage of a wider coverage of the emission plume and a more flexible sampling strategy which can be adapted depending on the wind direction. In recent years tracer dispersion methods were developed and became more widely used (Czepiel et al., 1996; Galle et al., 2001; Foster-Wittig et al., 2015; Mønster et al., 2015). In this approach a tracer is released at the source and sampled downwind together with the target gas. Initially, sulfur hexafluoride (SF_6) (Czepiel et al., 1996) and N_2O (Galle et al., 2001) were used as tracers, which are greenhouse gases themselves. Mønster et al. (2014) and Foster-Wittig et al. (2015) used acetylene as a tracer, which was co-measured with CH_4 with cavity ring-down spectroscopy (CRDS). This technique provides accurate measurements of CH_4 emissions of landfills and can also be applied to divide between several sources in one area by using an additional tracer (Scheutz et al., 2011; Mønster et al., 2014). A requirement for this method is accessibility downwind of the site for sampling the plume, and the time span that can be covered is limited. The use of an unmanned aerial system (UAS) as a mobile sampling platform has been carefully assessed recently (Allen et al., 2014, 2015). Present challenges are finding high-precision CH_4 sensors that can be installed and operated on a UAS and developing a safe flight pattern covering the up- and downwind signal (Allen et al., 2015).

Atmospheric dispersion models appear as a useful tool for investigation of emissions from landfills and other area

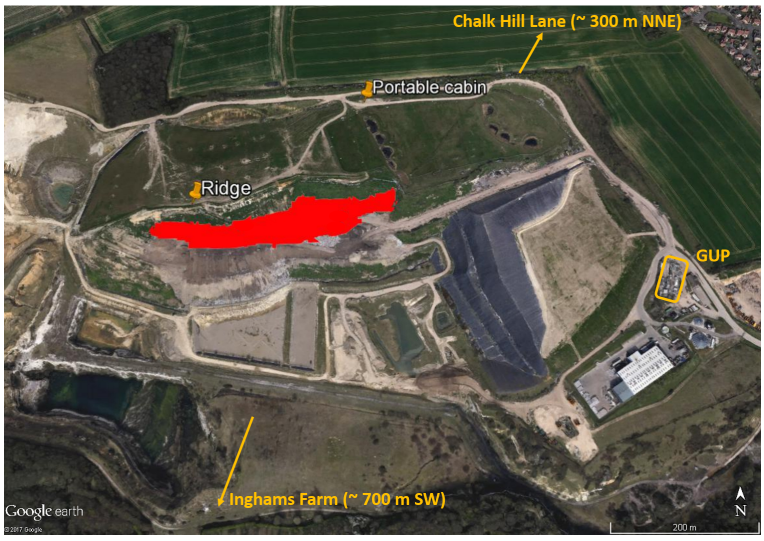

Figure 1. Bird's eye view of the landfill site with the active site coloured in red in the centre. The portable cabin with the FTIR is located at the north edge of the landfill site. Additional instrumentation was located at the ridge above the active site. A GC used for background measurements was situated about 700 m SW off-site at Inghams Farm, and a CRDS was operated on Chalk Hill Lane about 300 m NNE. The entry to the site with the weighbridge and the gas utilisation plant are at the east side.

sources. Delkash et al. (2016) used a forward model to analyse the effects of wind on short-term variations in landfill emissions in combination with a tracer method. The use of backward Lagrangian modelling for estimating gaseous emissions from a known area source in flat terrain with a single sensor has been described in detail by Flesch et al. (1995, 2004). This technique was also applied by Bell et al. (2017) for monitoring ammonia emissions from grazing cattle. Hrad et al. (2014) used backward Lagrangian modelling to estimate emissions from an open windrow composting plant. They found an agreement of 10 to 30 % in an intercomparison with tracer release experiments over 5 days. Zhu et al. (2013) and Riddick et al. (2016) applied this method for monitoring CH_4 emissions from a landfill site.

The GAUGE (Greenhouse gAs Uk and Global Emissions) project aims for a better understanding and quantification of the UK GHG budget to support GHG emission reduction measures. In this context a 2-week field campaign between 4 and 15 August 2014 at a landfill site north of Ipswich, UK, was conducted as part of the GAUGE project to improve our understanding of landfill emissions and to investigate different methods for flux quantification. Here, we present simultaneous and continuous observation of CO_2 and CH_4 with in situ Fourier-transform infrared (FTIR) spectroscopy at this landfill site. The use of the same kind of instrument for measurements of emissions from a waste water treatment plant was presented by Yver Kwok et al. (2015) in combination with floating chambers on the basins.

The application of a computational fluid dynamics (CFD) model to the point measurements for estimating CH_4 fluxes is described and assessed. For complex terrains such as a landfill site CFD models are expected to be more useful compared to Gaussian tools (Mazzoldi et al., 2008). Topographic information can be used by the CFD model to adapt to a more complex terrain, where backward Lagrangian models work best on a horizontally homogeneous surface layer (Flesch et al., 2004). This approach has the potential to provide a continuous data set for flux derivation from one set of CFD runs. It also offers the opportunity to identify and divide between different source areas.

In the following, the measurements during the field campaign are described and emission ratios are calculated initially to assess the influence of landfill emissions on the sampled air. Then the method for flux calculations with the CFD model outputs is presented. Emissions from the active site and a secondary source area are discussed.

2 Materials and methods

2.1 Experimental site

The landfill site under study is located in Great Blakenham near Ipswich (Fig. 1). In operation since 1992, it accepts a range of domestic and commercial/industrial waste and occupies approximately 330 000 m^2. The oldest part of the site, towards the north, is capped with a high-density polyethylene (HDPE) liner and covered with at least 1 m of restoration soils. East of the active area is a completed cell, which is temporarily capped with an HDPE only. The operational area (red area in Fig. 1) is located at a lower level to the centre of the site. Waste is deposited in this area on weekdays and Saturday mornings. The active waste is covered at the end of

each day with a daily cover comprising soils and other inert materials. The site is equipped with an active gas control system comprising a network of gas extraction wells and associated pipe work connected to four nominally 1 MW_e LFG engines. Two high-temperature enclosed flares provide backup LFG control. All engines and flares are located in the gas utilisation plant (GUP) towards the southeastern end of the site.

Measurements were carried out at different locations on the landfill site. With a focus on emissions from the active area, the main instrument used in this study (FTIR) was accommodated in a portable cabin at the north end of the landfill site about 320 m downwind from there. Further instrumentation was located on the ridge above the active site, including meteorological instruments and another greenhouse gas analyser to measure CO_2 and CH_4. This greenhouse gas analyser was either connected to a set of surface flux chambers or set up for sampling ambient air. A gas chromatograph (GC) for CH_4 measurements was installed at Inghams Farm approximately 700 m southwest of the landfill site. A cavity ring-down spectrometer measuring CH_4, CO_2, CO and H_2O was located about 300 m northeast of the landfill on Chalk Hill Lane (Riddick et al., 2016).

2.2 FTIR

The instrument deployed at the northern edge of the landfill site in the portable cabin was a Spectronus Trace Gas and Isotope Analyser by Ecotech (Knoxfield, Australia), hereafter referred to as FTIR. Detailed descriptions of the FTIR can be found in Griffith et al. (2012) and Hammer et al. (2013). The built-in spectrometer is a Bruker IR cube with a range of 2000 to 7800 cm^{-1} and a resolution of 1.0 cm^{-1}. The spectrometer measures the absorption of the air sample in a 3.5 L White cell. With a flow rate of 1 L min^{-1}, the standard sampling time of 3 min corresponds closely to a sample exchange in the cell. Before the sample enters the cell it passes a Nafion dryer and a chemical dryer filled with magnesium perchlorate. Mole fractions of CO_2, CH_4, CO and N_2O, as well as the $^{13}CO_2$ isotopologue, are retrieved by software provided with the instrument. For this study we focus on the CH_4 measurements. Background spectra were recorded shortly before and during the campaign. A two-point calibration was conducted on the last day of the measuring period with two primary standards of different mole fractions. They were calibrated at the Empa – Swiss Federal Laboratories for Materials Science and Technology, Dübendorf, Switzerland, relative to the World Meteorological Organization (WMO) scale (WMO-CH_4-X2004A, WMO-CO_2-X2007, WMO-N_2O-X2006A, WMO-CO-X2014). For stability monitoring, a target gas was measured daily. As no clear trend was observed with the target gas measurements, no corrections were applied, but the observed variation was considered for estimation of the uncertainty. The combined uncertainty based on calibration with the primary gas standards and the target gas measurements is 0.44 ppm for CO_2 and 1.93 ppb for CH_4. The inlet for the FTIR was fixed to a tripod in front of the portable cabin around 2 m above ground. Air was sampled through Teflon tubing using one of the four sampling ports of the FTIR with a flow of 1 L min^{-1}. A filter attached to the tubing prevented particles from entering the instrument. Irregularities in the power supply caused a delayed start of the measurements and another disruption later on. Additionally, a software error caused another gap in the data.

2.3 Background measurements and further instrumentation

To quantify the landfill CH_4 emissions, the background level of CH_4 needs to be distinguished from the enhanced CH_4 concentration related to the landfill emissions. Measurements by the University of Cambridge with a 200 series Ellutia GC-FID (gas chromatography–flame ionisation detector) about 700 m off-site to the southeast were used as background for southerly wind directions. For wind coming from the north, measurements of a Picarro cavity ring-down spectrometer, located northeast of the landfill site, are used as background. The set-up of both instruments is described in Riddick et al. (2016). Data were available with a time resolution of 15 min and uncertainty of 0.8 %. Additional measurements of CO_2 and CH_4 were taken occasionally at the ridge by the University of Manchester with an Ultraportable Greenhouse Gas Analyzer (UGGA) by Los Gatos Research (Mountain View, California, USA), hereafter referred to as UGGA, which is based on off-axis integrated-cavity output spectroscopy (Off-Axis ICOS). A detailed description of this technique can be found in Baer et al. (2002). An uncertainty of 1 % for the retrieved mole fractions is stated by the manufacturer. This has been verified by subsequent laboratory calibrations, where the agreement between the UGGA and a WMO-traceable cylinder has been within this nominal uncertainty. Wind speed and direction were recorded at the ridge at 2 m elevation above ground with a WindMaster Pro 3-D sonic anemometer by Gill Instruments (New Milton, UK) throughout the campaign. The accuracy for the wind speed is 1 % RMS (root mean square) at 12 m s^{-1} and 0.5° in wind direction for typical wind speeds.

2.4 CFD model

The gas dispersion from the landfill surface was calculated with a CFD model using the OpenFOAM (Open Field Operation and Manipulation) open source software platform (freely available at http://www.openfoam.com). CFD models use fluid dynamics equations constrained by boundary conditions that are solved numerically to calculate the behaviour of a fluid such as air within a particular domain (here the landfill terrain). CFD models require a complex parameterisation compared to traditional Gaussian dispersion models,

but they have been shown to provide increased accuracy over complex terrain (Buccolieri and Sabatino, 2011), which can be considered to be the case over the landfill site. Resolving three-dimensional distributions of wind flow and gas concentration in the modelling domain on small scales makes them an attractive choice compared to Lagrangian dispersion models (Leelőssy et al., 2014). The CFD model presented in this study has previously been evaluated by a comparison exercise against a wind tunnel experiment (Jeanjean et al., 2015) and measurements from an urban monitoring station (Jeanjean et al., 2017). As a result of this comparison it was shown that a model accuracy of 30 to 40 % can be achieved. This represents a slight amelioration with respect to traditional Gaussian dispersion modelling.

2.4.1 Landfill site survey and computational domain

This study made use of a digital surface model, which was obtained from a terrestrial lidar (Light Detection and Ranging) survey, collected using a terrestrial laser scanner (Riegl LMSZ420i). The data were collected with a point spacing of between 20 and 50 cm, depending on the accessibility of the landfill site. Lidar scans from five locations around the site were then merged into a single surface model element using the Innovmetric PolyWorks software. The landfill surface data were finally georeferenced with a differential GPS (Global Positioning System, Trimble Pro 6T) which provides a sub-metre accuracy for global georeferencing. A more detailed summary of the use and processing of this kind of lidar data can be found in Hodgetts (2013).

The resulting digital surface model was then resampled into a 1 m grid, which in turn was extended using a 5.0 m digital elevation model from the Ordnance Survey (UK government agency responsible for topographic survey and mapping of Great Britain) to extend the studied area as shown in Fig. 5a. The terrain was then incorporated as a three-dimensional file to build a computational grid in the OpenFOAM CFD software.

The total number of cells used for the simulation numbered 142 000. The boundaries used for the mesh are (given in metres in the British National Grid, minimum to maximum) $X = [610\,350, 611\,650]$, $Y = [249\,700, 250\,500]$, $Z = [0, 500]$. The initial cells of the domain were assigned a dimension of 30 m. The cells corresponding to the terrain (ground) were assigned a size of 2 m and were kept constant up to 30 m away from the ground. Their resolution was then coarsened beyond 30 m with a maximum expansion ratio of 1.2.

2.4.2 Numerical settings

The wind flow in the CFD model was calculated with the Reynolds-averaged Navier–Stokes (RANS) k-ϵ model (Launder et al., 1975). Following a parameterisation for a neutral atmospheric boundary layer in Hargreaves and Wright (2007), the mean velocity boundary flow and the turbulent dissipation were set up to follow a logarithmic law using the ABLInletVelocity U (Eq. 1) and ABLInletEpsilon ϵ (Eq. 2) utilities in OpenFOAM such that

$$U = \frac{U^*}{K} \ln\left(\frac{z + z_0}{z_0}\right) \tag{1}$$

and

$$\epsilon = \frac{U^{*3}}{Kz}\left(1 - \frac{z}{\delta}\right), \tag{2}$$

where K is the von Kármán's constant, z is the height coordinate (m), z_0 is the roughness length (m), δ is the boundary layer depth (m) and U^* is the frictional velocity ($m\,s^{-1}$). The turbulent kinetic energy k was set up as follows:

$$k = \frac{U^{*2}}{\sqrt{C_\mu}}, \tag{3}$$

where $C_\mu = 0.09$ is a k-ϵ constant.

The top boundary condition of the domain was set up as a symmetry condition. The inlets, where air enters the domain, and outlets, where air leaves the domain, were adjusted depending on the simulated wind conditions. For example, to simulate a southeasterly wind, the two inlets would be the south and eastern sides of the landfill domain and the outlets would be the northern and western sides. A wall function was used for the ground to reproduce the landfill surface roughness. A roughness length value of 0.03 m was used to model the landfill terrain. This roughness length value corresponds to an open terrain with grass and a few isolated obstacles (WMO, 2008).

The dispersion of emissions from the landfill site was simulated using a passive scalar transport equation defined such that

$$\frac{\partial C}{\partial t} + \nabla(UC) = \nabla^2\left((D + K_e)C\right), \tag{4}$$

where C is the concentration of CH_4 ($g\,m^{-3}$), U is the fluid velocity ($m\,s^{-1}$), D is the molecular diffusion coefficient ($m^2\,s^{-1}$) and K_e is the eddy diffusion coefficient ($m^2\,s^{-1}$). The eddy diffusion coefficient can be expressed as $K_e = \mu_t / Sc_t$, where μ_t is the eddy viscosity or turbulent viscosity ($m^2\,s^{-1}$) and Sc_t is the turbulent Schmidt number. Sc_t values range between 0.3 and 1.3 (Tominaga and Stathopoulos, 2007). A suitable Sc_t for this study was determined in a tracer release experiment on-site conducted by the University of Bristol. For details see Jeanjean (2017). Perfluoromethylcyclohexane (PMCH) was released from a point source on the southern edge of the landfill site. While the wind was coming from a southern direction, four bags were sampled on the northern part of the landfill. A relatively common value of $Sc_t = 0.7$ appeared to be the best choice to represent the measured concentrations of the bag samples. Riddle et al. (2004) also used $Sc_t = 0.7$ for CFD simulations over agricultural land.

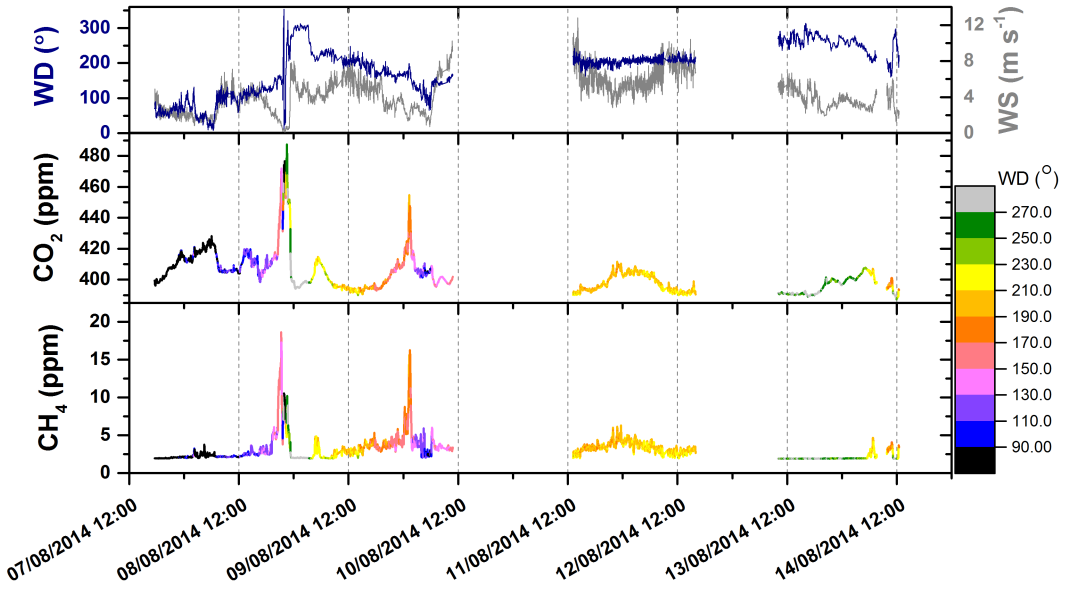

Figure 2. Time series of wind speed (WS, grey) and direction (WD, dark blue) in the top panel and of CO_2 and CH_4 colour coded with the wind direction. Black and grey refer to background air (270 to 90°), orange and yellow indicate air coming from the active site, and blue to light-pink and green colours mark transitional periods.

2.4.3 Model limitations

A RANS CFD model provides a steady state view of the reality, which corresponds to a fixed picture of the wind flow and pollutant concentrations. In real life, the wind is oscillating in strength and directions and CH_4 concentrations are highly variable following wind and landfill emission patterns. This study accounts for a calculated 3 min averaged concentration of CH_4, and the use of this estimation introduces limitations in terms of temporal variation. The model used here was best suited for constant wind directions; the RANS CFD model should be used with care when wind conditions are variable.

Thermal effects can affect gas dispersion as well, especially for large temperature gradients and low wind speeds. For wind speeds greater than $2\,m\,s^{-1}$, previous studies in an urban environment in winter have noted that wind dynamics are predominant over thermal effects, which can then be neglected (Parra et al., 2010; Santiago et al., 2017). The authors are not aware of any studies which quantify thermal effects on CFD modelling in rural environments or on a landfill site. In this study, thermal effects were not taken into account in the CFD model and remain a source of uncertainty. However, since only wind speeds greater than $2\,m\,s^{-1}$ were used, the influence of thermal effects should be minimised.

Despite these limitations, CFD dispersion models are currently one of the most advanced tools available for researchers to model gas dispersion over non-uniform terrain. They are most suited for a well-developed turbulence regime when stable wind directions and wind speed conditions are met.

3 Results and discussion

The landfill campaign took place between 4 and 15 August 2014. Initially, wind was coming from the northeast with relatively low wind speeds (see Fig. 2, top panel). On 8 and 10 August the wind came mainly from east to southeast, while the dominant wind direction on 9 and 11 to 12 August was from the south. At the end of the campaign the wind shifted more towards a westerly wind. The most frequent wind direction was around 210° (0/360° corresponding to north), and wind speeds ranged from 0.1 to $13\,m\,s^{-1}$. The time series of measured CH_4 and CO_2 mole fractions are shown in Fig. 2 in the lower two panels colour coded with the wind direction. The active site lies roughly between 170 and 240° as seen from the portable cabin. CH_4 values drop to background levels during measurements for air from the northern semicircle (black and grey lines in Fig. 2); in the CO_2 data a constantly low background value does not become apparent. High peaks in both gases appear before midnight on 8 August, when wind speeds were dropping to near zero, and in the following night for wind directions of 150 to 190°, which are only partially influenced by the active site. Two periods with wind constantly coming from the active area occurred during the course of the campaign: 9 and 11 to 12 August. Air influenced by the active site was also measured during the night of 9 to 10 August until after midnight and on 14 August from the early morning hours to noon. These periods were less stable in wind direction compared to the former time periods.

Much higher mole fractions with up to 700 ppm CO_2 and over 100 ppm CH_4 were observed by the UGGA at the ridge.

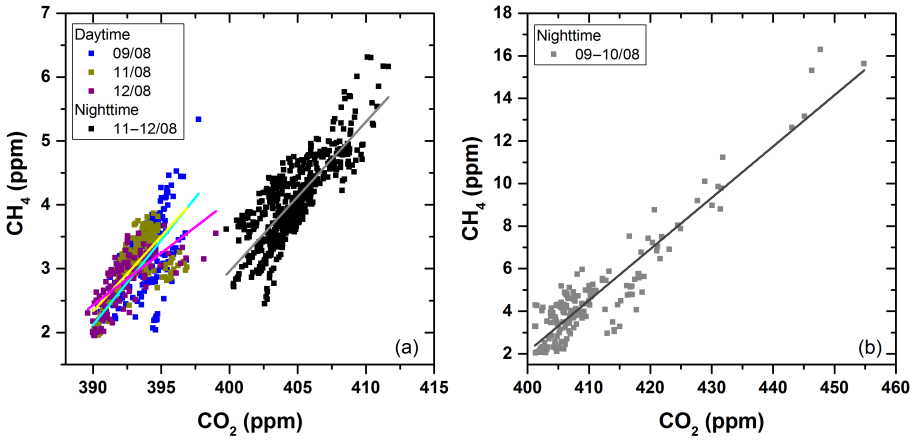

Figure 3. Determination of the enhancement factor as the linear regression slope of χ_{CH_4} vs. χ_{CO_2} separately for 3 days (09:00 to 18:00 UTC) and 2 nights (21:00 to 06:00 UTC) influenced by air from the active site. Data are shown in two separate panels to account for the different scales.

These particularly high values were measured before the FTIR measurements were started, so a direct comparison here is not possible. Towards the end of the campaign both instruments were operated at the same time. Mole fractions measured then were much lower compared to the beginning, but values at the ridge were still enhanced compared to the portable cabin. Chamber measurements along the south side of the ridge leading down to the active site showed that the cover of the old landfill part was not leak tight and allowed for additional significant emissions. CH_4 migrating underneath the landfill cap can leak out at places where the landfill cover is interrupted, e.g. at the edge of a side slope or through cracks in the cap. This is a common issue at landfill sites and highly variable emissions from these hotspots have been reported (Di Trapani et al., 2013; Rachor et al., 2013; Gonzalez-Valencia et al., 2016).

Although they contribute to the total GHG emissions of the landfill, measurements within the close proximity of those hotspots are not suitable for estimation of emissions from the active site. High temporal variability and spatial inhomogeneity would result in non representative fluxes. Hence, the application of the CFD model to the ridge measurements is not presented here. Emissions derived from measurements in greater distance to these hotspots can include their contribution into bulk emission estimates (see Sect. 3.4).

3.1 Emission ratios

The ratio of ppm CH_4 per ppm CO_2 at the location of the emission source is often referred to as an emission ratio and is given here in ppm ppm^{-1} for simplicity. It can provide insights into the degree of CH_4 oxidation at landfill sites (Gebert et al., 2011; Pratt et al., 2013). Under anaerobic conditions the landfill gas is typically enriched in CH_4 and results in ratios of 1.2 to 1.5 ppm ppm^{-1} for CH_4 to CO_2 (Lohila et al., 2007; Gebert et al., 2011). On-site continuous monitoring undertaken in a borehole by Ground-Gas Solutions (GGS) detected LFG ranging from 59 to 67 % CH_4 and 31 to 42 % CO_2, which results in a mean ratio of 1.8 ppm ppm^{-1}.

As the FTIR is not directly located at the source, the observed signals χ_{meas} of CH_4 and CO_2 are the combination of the background and the enhanced mixing ratio ($\Delta\chi = \chi_{meas} - \chi_{bg}$) from the active site. From that, the enhancement factor (EF) $= \Delta CH_4/\Delta CO_2$ is determined (Lefer et al., 1994), which corresponds to the emission ratio as long as there are no additional sources or sinks along the transport pathway. Here we determine the EF directly from the regression slope of χ_{CH_4} vs. χ_{CO_2} (Fig. 3) without prior background subtraction, as described in Yokelson et al. (2013), because background values for CO_2 were not available for the whole measurement period. Data for periods influenced by the active site are plotted separately for daytime (09:00 to 18:00 UTC) and nighttime (21:00 to 06:00 UTC) as the background of CH_4 and CO_2 is expected to change during the course of a day – that way EF is derived from data with comparable background values. Data in between the day- and nighttimes showed a gradual shift in background concentration, which leads to an artificially lower EF.

Results for the EFs are given in Table 1. A similar slope was observed for all 3 days and the 2 nights. The EFs are in the range of 0.16 to 0.27 ppm ppm^{-1} with a mean of 0.23 ± 0.04 ppm ppm^{-1}. There is a correlation in all cases with R^2 between 0.393 and 0.857. The lowest correlation coefficient was observed for 9 August 2014, when the wind field was less stable and covered a wider range in wind directions than on the other days. Compared to air masses coming from the north, CH_4 is enhanced, but the EF is significantly lower than would be expected from landfill gas from underneath the cover. This suggest that the sampled air during these phases had picked up emissions from the active site,

Table 1. EF given as ppm CH_4 per ppm CO_2 with fit uncertainty and R^2 as determined from the slope of the regression from the correlation of CH_4 to CO_2 measured at the portable cabin for daytime (09:00 to 18:00 UTC) and nighttime (21:00 to 06:00 UTC) separately.

Date	Day/ night	EF (ppm ppm^{-1})	R^2
9 August	Day	0.266 ± 0.026	0.393
11 August	Day	0.235 ± 0.012	0.572
12 August	Day	0.163 ± 0.015	0.499
9 to 10 August	Night	0.241 ± 0.007	0.857
11 to 12 August	Night	0.234 ± 0.007	0.655

which is enriched with CH_4 but due to the exposure to air is more oxidised than landfill gas.

Daytime EF measured at the ridge, closer to the active site, with the UGGA ranged from 0.42 to 0.54 ppm ppm^{-1}. Compared to the EFs observed at the portable cabin, they show a higher CH_4 content but can still be interpreted as being representative of waste degradation under mainly aerobic conditions. Processes at the surface of a landfill site can alter the CO_2 concentration (Scheutz et al., 2009). Hence, interpretation of the EF as an estimate for the emission ratio with regard to the degree of CH_4 oxidation can be difficult. The difference can be explained by additional CO_2, which was taken up by the air masses during the transport over the capped area between the ridge and the portable cabin. Closed chamber measurements by GGS found a CO_2 flux of 0.1587 mg m^{-2} s^{-1} in this area, but no significant CH_4 emissions.

3.2 Distribution of ΔCH_4

The distribution of ΔCH_4, the enhanced concentration over the background value, over the whole range in wind direction as seen from the portable cabin is shown in Fig. 4. The CH_4 data were averaged over 15 min, and the background CH_4 concentration was subtracted by using the GC data for wind directions from the south and the Picarro data for wind coming from the north. In the morning of 8 August, the wind direction changed rapidly from around 20 to 100° and high CH_4 concentrations were observed with the GC. This resulted in negative values of ΔCH_4 when subtracting the background from the FTIR data. Between 120 and 220° CH_4 levels are clearly elevated when wind is passing the landfill site before reaching the portable cabin. Outside this range CH_4 concentrations are at background levels. Highest concentrations are observed during low wind speeds when emitted gases accumulate. Generally, the wind speed was higher for wind directions above 150°. Two maxima in ΔCH_4 at around 140 and 200° stand out. The focus of this study is the elevated ΔCH_4 at around 200° (grey shaded area in Fig. 4) to assess emissions from the active site, which was assumed

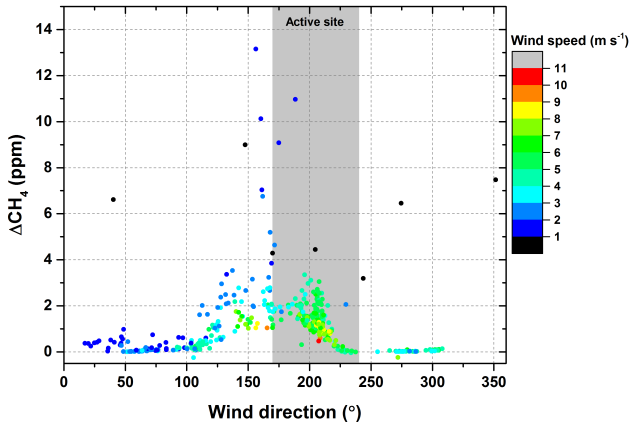

Figure 4. Distribution of ΔCH_4 with wind direction and colour coded with the wind speed based on 15 min averages. The wind direction range of the active site is marked in grey.

to be the main emitting part of the landfill. Figure 4 indicates that further emissions are coming from other parts of the landfill as well. The maximum at 140° is from air passing the GUP close to the weighbridge of the landfill site and the fully filled but not yet fully restored area.

3.3 Application of CFD model to the in situ data for flux calculations

The CFD model is applied to simulate the distribution of CH_4 concentrations emitted from the active site of the landfill at the point of measurement for different meteorological scenarios. Figure 5a shows a 1 m grid-resolved topographic map from the lidar survey of the landfill site. The red area in the topographic map marks the active site of the landfill site. Over the estimated area of the active site of $A = 17\,823$ m^2, a constant emission f_{Source} normalised to 1 g s^{-1} is set. Figure 5b shows the simulated concentration of the emitted compounds by the CFD model for the position of the portable cabin at 2 m height depending on the wind direction for four different wind speeds. The units used by the CFD model correspond to a mass concentration C_{Source} in g m^{-3}, which is converted to mole fractions χ_{Source} for CH_4 with a molar mass of $M_{CH_4} = 16.04$ g mol^{-1} for comparison with the measurements (Eq. 5). The molar concentration of air c_{Air} is 40.34 mol m^{-3}.

$$\chi_{\mathrm{Source}} = \frac{C_{\mathrm{Source}}}{c_{\mathrm{Air}} \cdot M_{CH_4}} \tag{5}$$

The ratio of measured, χ_{FTIR}, to modelled mole fraction, χ_{source}, is used to scale the normalised emission and calculate the CH_4 flux with Eq. (6).

$$F_{CH_4} = \frac{f_{\mathrm{Source}} \cdot \chi_{\mathrm{FTIR}}}{A \cdot \chi_{\mathrm{Source}}} \tag{6}$$

The CFD model calculates only the enhancement above the background concentration based on the defined emis-

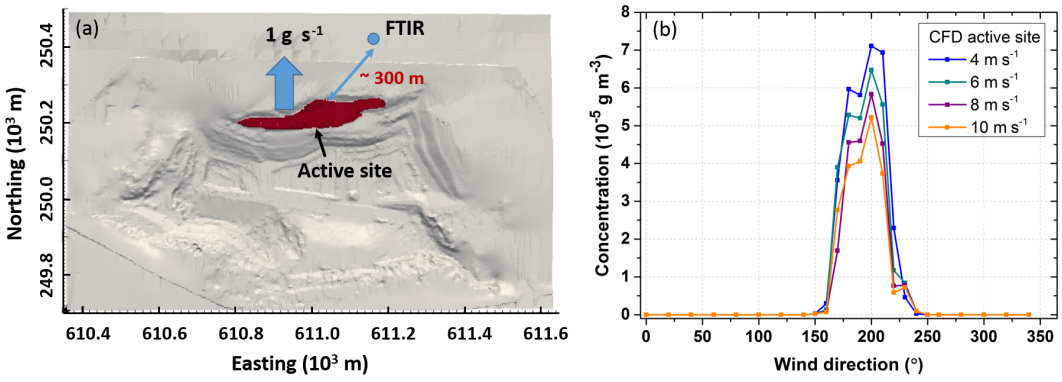

Figure 5. The emission area used for the CFD approach is marked in red on the topographic map embedded in the British National Grid coordinate system **(a)**. The results of the CFD model for the position of the FTIR measurement site are shown in **(b)**.

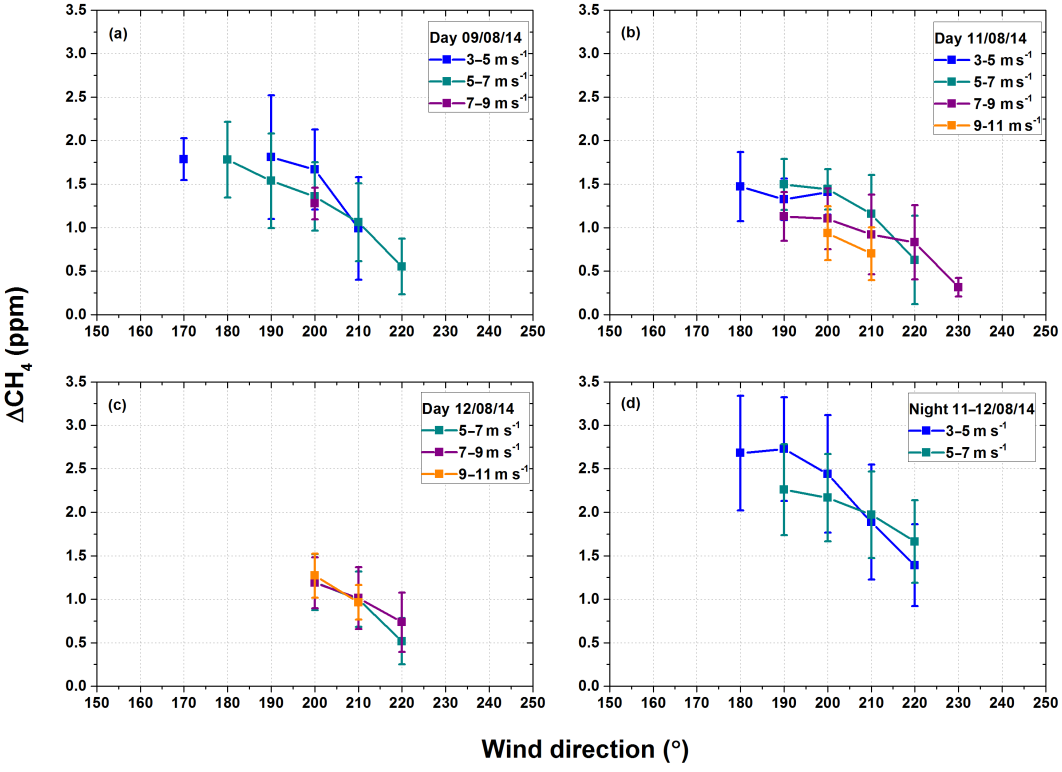

Figure 6. ΔCH_4 averaged bin wise, matching the CFD outputs for each day **(a–c)** and the 1 night **(d)** with wind coming from the active site. The standard deviation is plotted as error bars. Data are only shown for more than five data points per bin.

sions f_{Source}. Therefore, the outputs correspond to the enhanced mole fraction ΔCH_4 in Eq. (6). As before for the enhancement ratios, data were analysed separately for day and night for periods with air mainly coming from the active site (daytime: 9, 11 and 12 August; and nighttime: 11 to 12 August). The CH_4 background values were calculated from the off-site GC measurements as the mean over these periods and are given in Table 2.

The CFD model results refer to wind speeds (WSs) of 4, 6, 8 and 10 m s^{-1} for all wind directions (WDs) and are given as WS–WD pairs of 10° between 140 and 260 and 20° elsewhere. Taking this into account, the mean of the FTIR data was calculated around these model output pairs. Mean enhanced mole fractions and their standard deviations of CH_4 with at least five data points per bin are shown in Fig. 6. High CH_4 concentrations are observed in the range of 170 to 200°, decreasing towards more westerly wind directions. On these days no significant amount of data for wind directions below 170° was collected. Especially on 11 August and during the night of 11 to 12 August, a distinction of the data

Table 2. Mean CH_4 fluxes and standard deviations for the ensemble of derived fluxes for each day and night calculated from the binned FTIR data with the CFD results and the respective background values (BG). The uncertainty for each calculated flux value is estimated from error propagation based on the standard deviation of ΔCH_4 per bin and the model uncertainty (see main text for detail). The range of these uncertainties for each day and night is given in the last column.

Date	Day/ night	BG (ppm)	Flux ($mg\,m^{-2}\,s^{-1}$)	Uncert. flux (%)
9 August	Day	1.898	0.99 ± 0.39	40.4–44.9
11 August	Day	1.869	0.79 ± 0.12	40.6–43.2
12 August	Day	1.867	0.78 ± 0.11	40.6–41.9
11 to 12 August	Night	1.911	1.38 ± 0.26	41.8–43.6

based on the wind speed with higher values for lower wind speeds can be seen. Table 2 summarises the mean by day and night of the fluxes calculated for each bin of ΔCH_4 and their standard deviations, reflecting the spread of fluxes calculated for these periods. The respective background values are given as well. The uncertainty in percent is calculated for each derived flux value through error propagation from the model uncertainty of 40 % and the standard deviation of each binned ΔCH_4 value (as shown in Fig. 6). The range in uncertainty for each day and night is given in Table 2. The model uncertainty of 40 % is the main contribution to the uncertainty. Measurement uncertainties are significantly smaller and were not taken into account here.

For the different days the calculated fluxes are in good agreement. For the night a higher flux was found. The calculated fluxes given in Table 2 refer to wind directions below 220° only. The steep decline in concentration at 220° based on the CFD model results was not observed in the FTIR data. The fluxes inferred for this range are up to a factor of 6 higher. Additional emissions from hotspots along the side between the ridge and the active site, which initially were not taken into account by the CFD model, could cause the enhanced CH_4 concentrations from this direction.

Instead of calculating the flux for each WS–WD pair separately, the CFD outputs were also fitted to the FTIR data with a linear least-squares fit over all wind directions present for each day and night and wind speed using Eq. (7).

$$\chi_{\mathrm{FTIR},i} = \frac{f_{\mathrm{Source}} \cdot F_{\mathrm{CH_4}}}{A} \cdot \chi_{\mathrm{Source},i} \tag{7}$$

A robust fitting method using an M estimator to reduce the influence of outliers was also tested, but did not have a significant effect on the results. Hence, only the results from the linear least-squares fit are reported in the following (Table 3). The standard errors are the fit uncertainty of the coefficient. Inferred fluxes range from 0.66 to $0.92\,mg\,m^{-2}\,s^{-1}$ during daytime and 1.37 to $1.39\,mg\,m^{-2}\,s^{-1}$ at night. When all daytime data are fitted together an overall flux of $(0.83 \pm 0.04)\,mg\,m^{-2}\,s^{-1}$ is obtained. This results in CH_4 emissions of $53.3\,kg\,h^{-1}$ over the active site.

It should be noted that the CFD model turbulence mixing parameters were optimised to match the bag samples of the tracer release experiment. Hence, the CFD outputs correspond to daytime conditions, and fluxes calculated for nighttime need to be used with care but are included here for completeness. Generally, it can not be predicted how the CFD output would change with decreased turbulence, as it would be the case during night, as it highly depends on the location of the measurement and the meteorological conditions. Higher CH_4 emissions at night could also be explained with a decrease in temperature and a reduced activity of CH_4-oxidising bacteria (Scheutz et al., 2009). A small inverse relationship between temperature and CH_4 emissions at this landfill site was also observed by Riddick et al. (2016). Additionally, the fact that activity on the open site, moving vehicles and deposition of new waste, only takes place during the day could contribute to a diurnal pattern in landfill emissions by introducing oxygen-rich air into the surface layer of waste.

Enhancements in CH_4 (ΔCH_4) simulated from the inferred fluxes (Table 3) are shown in Fig. 7 together with the in situ data. At around 200° the measurements are well represented by the model, but model estimates were found to be lower for other wind directions. This is mainly the case for low wind speeds, where more CH_4 can accumulate, and wind directions further southeast.

3.4 Inclusion of an additional source area

As described in the previous section, the CFD model results in a steep decline in simulated CH_4 concentration at wind directions of 220° and further west, while measurements are still enhanced. No CH_4 emissions were observed on top of the restored section of the landfill site between the ridge and the portable cabin, but emission hotspots were detected on the south side of the ridge above the active site, hereafter referred to as side area (see light-pink area in Fig. 8a). Thus, we have included a secondary source area A_{side} in our analysis, estimated to be $26\,400\,m^2$. Gaps in the top liner along the side allow for CH_4 to escape underneath a soil cover with some vegetation. These emissions are directly adjacent to the emissions from the active site and are thereby also detected by the FTIR for wind coming from the south to southwest. The emission strength compared to the active site is unknown and can be expected to be highly variable (Rachor et al., 2013). To take these into account, a second CFD run for the described area as emission source was set up. For a normalised source flux of $f_{\mathrm{source}} = 1\,g\,s^{-1}$, concentration distributions as shown in Fig. 8b are modelled.

Flesch et al. (2009) discussed the requirement of having two sensors in different places for a two-source problem. However, they also describe the possibility of solving the problem with a single sensor, if the range in meteorologi-

Table 3. Results of a linear least-squares fit of the CFD model to the in situ data. CH_4 fluxes were fitted for each day and night and wind speeds separately. The standard error (SE) for the flux, adjusted R^2, the residual standard error (RSE) and degrees of freedom (df) are also shown.

Date	WS ($m\,s^{-1}$)	CH_4 flux ($mg\,m^{-2}\,s^{-1}$)	SE ($mg\,m^{-2}\,s^{-1}$)	Adj. R^2	RSE (ppm)	df
Day 9 August	4	0.89	0.22	0.805	0.71	3
	6	0.92	0.11	0.928	0.36	4
	8	0.80				0
Day 11 August	4	0.80	0.05	0.987	0.16	2
	6	0.87	0.10	0.950	0.27	3
	8	0.79	0.15	0.845	0.36	4
	10	0.66	0.01	0.999	0.02	1
Day 12 August	6	0.68	0.09	0.950	0.21	2
	8	0.80	0.20	0.833	0.41	2
	10	0.90	0.02	0.999	0.04	1
Night 11 to 12 August	4	1.37	0.16	0.936	0.58	4
	6	1.39	0.27	0.865	0.75	3

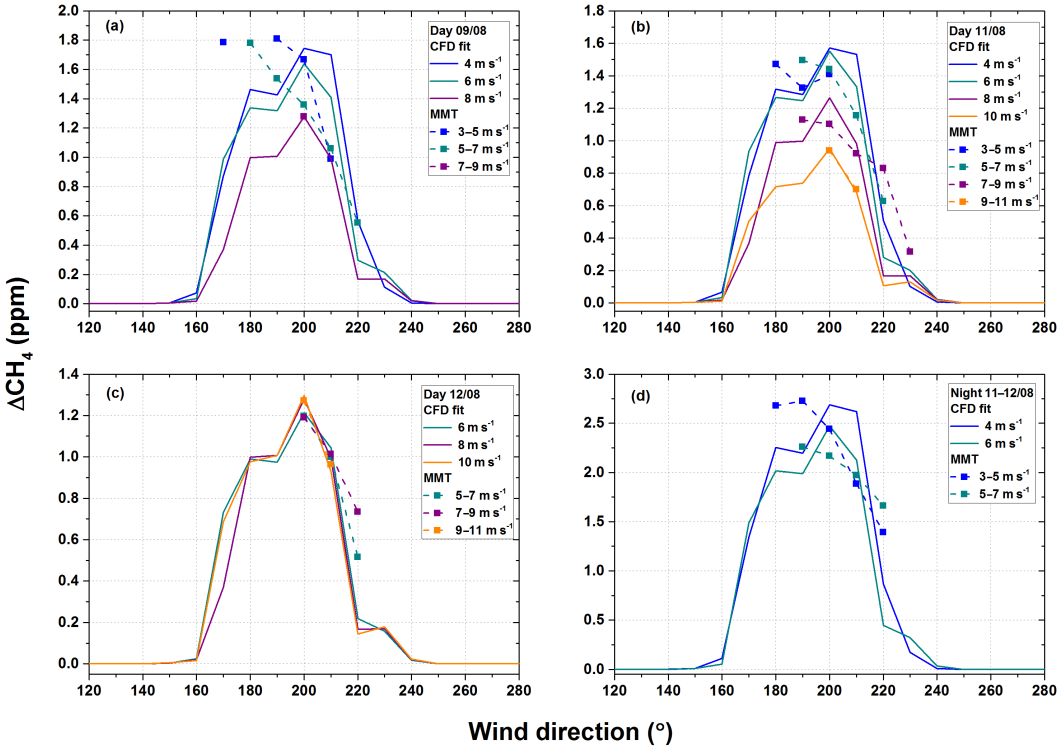

Figure 7. Measured (MMT) and simulated (CFD fit) ΔCH_4 based on linear fit of the CFD model to the FTIR data.

cal conditions is broad enough. Here, we have only one sensor available, but a range in wind speeds and direction for most days to cover different meteorological conditions. The modelled concentrations were combined with Eq. (8) to calculate the fluxes from both areas under the assumption that the measured CH_4 concentration is an accumulated signal of the emissions from the active site and the side.

$$\chi_{\mathrm{FTIR},i} = \frac{A_{\mathrm{active}} \cdot \chi_{\mathrm{active},i}}{f_{\mathrm{source}}} F_{\mathrm{active},i} + \frac{A_{\mathrm{side}} \cdot \chi_{\mathrm{side},i}}{f_{\mathrm{source}}} F_{\mathrm{side},i} \quad (8)$$

Equation (8) was applied in two ways. First, a linear least-squares fit was applied to the data of each day and night separately for each wind speed. Secondly, all daytime data were fitted with a linear least-squares fit together to derive

Table 4. Results of a linear least-squares fit from the combined CFD model outputs, for the active site and the side, to the in situ data. CH_4 fluxes were fitted for each day and night and for wind speeds separately. The standard error (SE) for the flux, adjusted R^2, the residual standard error (RSE) and degrees of freedom (df) are also shown.

Date	WS ($m\,s^{-1}$)	Active site CH_4 flux ($mg\,m^{-2}\,s^{-1}$)	SE	Side CH_4 flux ($mg\,m_{-2}\,s^{-1}$)	SE	Adj. R^2	RSE (ppm)	df
Day 9 August	6	0.84	0.16	0.22	0.30	0.919	0.38	3
Day 11 August	6	0.76	0.10	0.29	0.17	0.970	0.21	2
	8	0.65	0.13	0.36	0.17	0.919	0.26	3
Day 12 August	6	0.59	0.01	0.23	0.02	1.000	0.02	1
	8	0.60	0.04	0.56	0.06	0.996	0.07	1
Night 11 to 12 August	4	1.23	0.21	0.36	0.35	0.936	0.58	3
	6	1.03	0.12	0.97	0.19	0.985	0.25	2

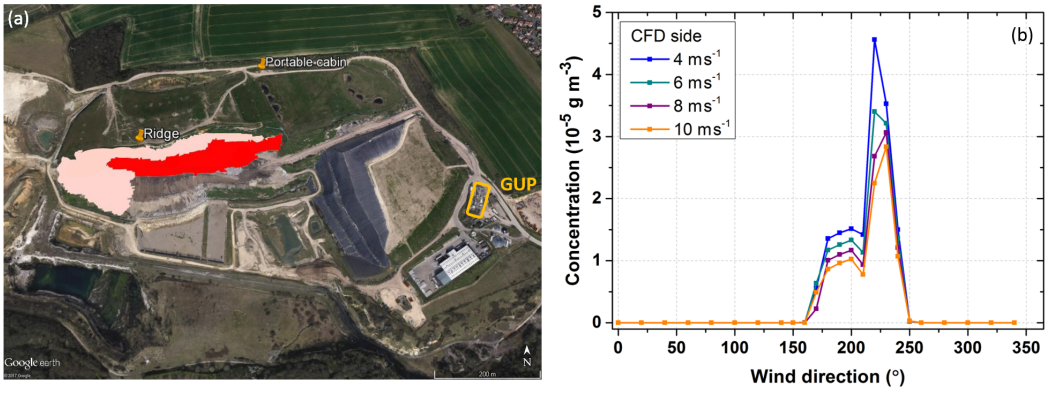

Figure 8. (a) Secondary source area (light pink) between the active site (red) and the ridge, and **(b)** CFD modelled concentration for the location of the FTIR measurements at the portable cabin based on the secondary source area only.

a mean flux. Fluxes from both source areas for each set of data are given in Table 4 together with their fit uncertainty as standard error and the residual standard error (RSE). The same robust fitting methods were applied again to take outliers into account. The results were found to be consistent with each other within the fit uncertainty. Hence, only results from the linear least-squares fit are reported.

The combined fit in cases where data are only available for the lower wind directions, such as for $4\,m\,s^{-1}$ on 9 and 11 August 2014, does not result in realistic coefficients for the fluxes and, in conjunction with their large errors, can not be considered as representative values. For wind speeds of $10\,m\,s^{-1}$ only two data points were available, i.e. zero degrees of freedom, and the fit assigned a much higher flux to the side area and only a minor contribution to the active site. Therefore, these fits were not further included. A longer measurement period would be of benefit to obtain data of a wider range in meteorological conditions.

Figure 9 shows simulated ΔCH_4 based on fluxes calculated from the separate fits with combined CFD runs in comparison with the measurements. At the peak wind direction both approaches show similar good agreement between the model and the measurements. Measured CH_4 concentrations at 220° are much better represented by the combined CFD model compared to the model run based on the active site only (Fig. 9). The mean RSE could be reduced from 0.42 to 0.25 ppm based on equivalent fits from 9 August ($6\,m\,s^{-1}$), 11 August (6 and $8\,m\,s^{-1}$), 12 August (6 and $8\,m\,s^{-1}$) and the night of 11 to 12 August 2014 (4 and $6\,m\,s^{-1}$). The mean fluxes from the same daytime data combined in one fit are $0.71 \pm 0.05\,mg\,m^{-2}\,s^{-1}$ for the active site and $0.32 \pm 0.08\,mg\,m^{-2}\,s^{-1}$ for the side. From this the overall emissions are $76.0\,kg\,h^{-1}$ over an area of $44\,223\,m^2$.

Another reason for a discrepancy between modelled and measured CH_4 mole fractions could be the parameterisation for the turbulence in the CFD model. A standard fixed turbulent dispersion parameterisation ($Sc_t = 0.7$, see Sect. 2.4.2) was used in OpenFOAM, assuming it to be the best description of the conditions at the landfill site. Similar parameterisation has been used in previous studies by Jeanjean et al.

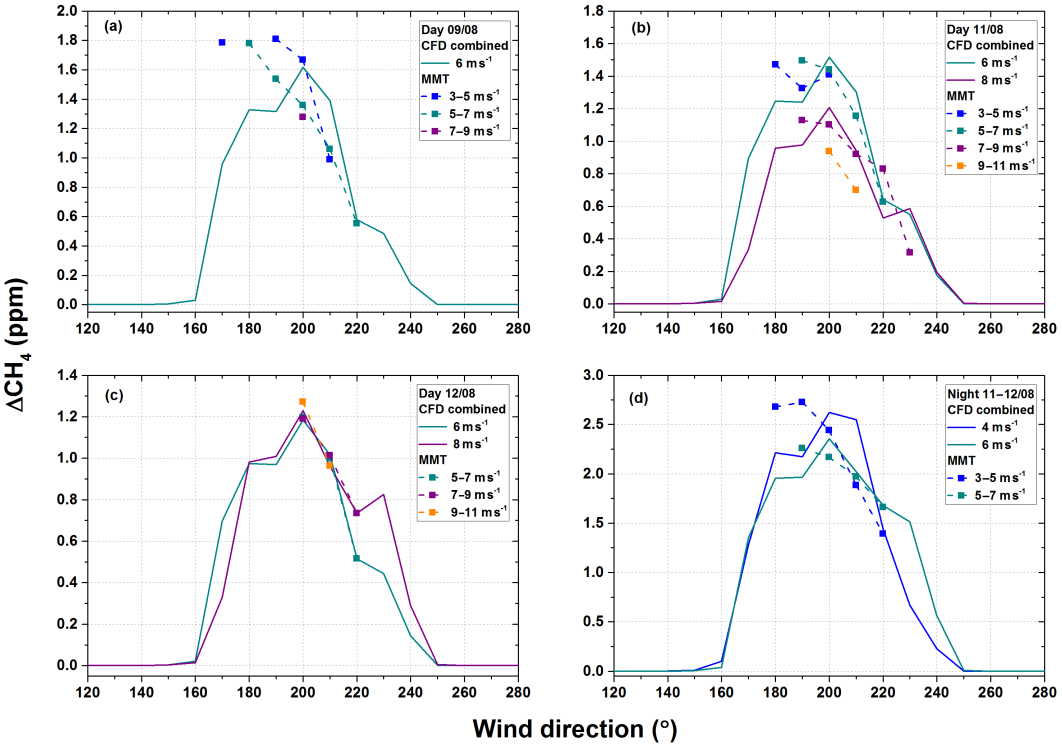

Figure 9. Measured (MMT) and simulated (CFD combined) ΔCH_4 based on a linear fit combining the CFD model for the active site and the side.

(2015, 2017) for evaluation of the CFD model. Over the landfill site, the turbulent mixing is likely to be variable with changes in roughness and topography across the site. This would subsequently lead to greater modelling errors. Fluctuations in wind speed and direction can lead to uncertainties in the results, if the aggregation time of the data is too short. This was addressed by averaging over at least five 3 min data points per bin for calculation of the fluxes (see Sect. 3.3).

3.5 Comparison to other flux estimations

Based on the CFD approach considering the active area, a mean daytime CH_4 flux of 0.83 mg m^{-2} s^{-1} was calculated, which corresponds to 53.3 kg h^{-1}. Including emissions from the side area results in an overall flux of 76.0 kg h^{-1} over a total area of 44 223 m^2. CH_4 fluxes from the landfill site were also measured by two other groups during the landfill campaign. Estimating the actual emitting area is a difficult task. While our focus was on the open active site, Riddick et al. (2016) included the surrounding area as well. Riddick et al. (2016) used an atmospheric inverse dispersion model to determine fluxes from the off-site CH_4 measurements between July and September 2014. They assume emissions to be only from the open site, which they estimate to be approximately 70 000 m^2. With 0.709 mg m^{-2} s^{-1} on average over day and night, they observed a CH_4 flux in good agreement with the one determined in this work. Based on the larger area, the total flux in Riddick et al. (2016) corresponds to 178.7 kg h^{-1}. They report an uncertainty of 42 % that is similar to our approach. Mønster and Scheutz (2015) applied a dynamic tracer dispersion method to estimate total CH_4 emissions from the landfill (total area: 330 000 m^2) between 5 and 12 August 2014. They derived fluxes in the range of 217 to 410 kg h^{-1} with a standard error of 14 to 42 % from six experiments in this period. CH_4 emissions estimated by the landfill site's owner are around 2230 t in 2014, which corresponds to an annual mean flux of 254.6 kg h^{-1}. This value is calculated from the total CH_4 as modelled based on waste input to the site and the LFG consumed by the power plant.

Compared to the other two methods we derived a lower CH_4 flux from the landfill site based on the on-site measurements at the portable cabin. The approaches of Riddick et al. (2016) and Mønster and Scheutz (2015) aim at quantifying the integrated signal of the whole landfill site, while our CFD approach focussed on emissions from the active site only (and separately the side area). Hence, fluxes obtained by these bulk emission methods are likely to be higher, including emissions from other areas, than the ones derived with the CFD approach. Indications for further emissions from wind directions towards the GUP and the temporarily capped completed cell in the southeast were visible in the CH_4 distribution measured with the FTIR (Fig. 4), but were not the subject of the present study. The definition of the source area is a crucial part for setting up the CFD simulation and needs to

be carefully assessed. When comparing fluxes inferred from different methods the source areas used need to be accounted for. As an advantage of the CFD approach, several source areas with different emission strength can be included.

4 Summary and conclusions

We presented a new approach to quantify CH_4 emissions from a defined source area at a landfill site. To this end, precise in situ measurements were combined with a CFD model. The CFD model only needs to be run once to cover the whole range of meteorological conditions and can then be applied to a series of continuous in situ measurements. Additionally, meteorological and background measurements are needed for application of the CFD model, which can easily be maintained over extended periods of time. The FTIR measurements can be conducted over a longer period without great effort and can thereby cover a wide range of various environmental conditions.

Consistent fluxes from the active site were found for 3 different days with southerly winds transporting air from the source area towards the portable cabin. Data from wind directions of 220° were not well reproduced by the CFD outputs for the active site only. Taking emissions from the side area between the active site and the ridge into account improved the agreement between measurements and model in this area. This shows that the emission source in the CFD model needs to be well defined. This is challenging for a heterogeneous terrain such as a landfill site, where several sources of CH_4 with different emission strength exist. This is where the CFD model demonstrates its strength by including the complex topography of the site. Chamber measurements or an initial walk-over survey with a small portable CH_4 sensor are valuable tools to characterise different parts of a landfill site and detect emission hotspots which are otherwise easily overseen by point measurements. It was discussed that measurements in the direct proximity of highly variable point sources such as landfill hotspots are not suitable for the approach with the CFD model. However, the position of the instrument should be close enough to detect a signal from the source areas from a range in wind direction in order to separate areas of different emission strength. The presented method could be improved by using multiple, spatially distributed sampling points. This could be achieved for future applications through the use of all four sample inlets of the FTIR to sample alternately from different points along the cross section of the plume. CFD results could be extracted for all sampling points without further modelling effort.

With our approach we estimated CH_4 emissions between 53 and 76 $\mathrm{kg\,h^{-1}}$ by the active site and surrounding area, depending on the area taken into account with the CFD model. These values represent only a snapshot of the landfill emissions based on the short measurement period. Longer-term or repeated measurements in different seasons would be needed to investigate emissions under different meteorological conditions and provide a more complete picture. The main contribution to the uncertainty of the derived emissions results from the limitations of the CFD model simulations. Compared to the total emission estimate from the landfill site's owner (254.6 $\mathrm{kg\,h^{-1}}$) and the bulk emission approaches by Riddick et al. (2016) (178.7 $\mathrm{kg\,h^{-1}}$) and Mønster and Scheutz (2015) (217 to 410 $\mathrm{kg\,h^{-1}}$), this assigns a smaller contribution to the active site and suggests additional significant CH_4 emissions from other parts of the site. Enhanced ΔCH_4 was observed for wind directions further east of the active site (Fig. 4), where the CFD model does not show any contribution from the active site. The presented study shows that the CFD approach can be used to assess the emission strength from a well-defined area in a complex terrain with several distinguishable emission sources.

Data availability. Data are available upon request from the authors.

Competing interests. Stewart Davies, employed by Viridor Waste Management Ltd. – the owner of the site under study, is co-author of this work in recognition of his expert technical guidance in planning fieldwork and for assisting with logistics on-site during the fieldwork and providing detailed information about the site. Neither he nor Viridor influenced the measurements, the modelling or the interpretation of the presented results. The authors declare that they have no other competing interests.

Acknowledgements. We thank NERC for their funding (NE/K002465/1 and NE/K002570/1) as part of the Greenhouse gAs Uk and Global Emissions (GAUGE) project. For technical and logistical support, we would like to thank the team of Viridor on-site. Thanks to Andrew Brunton and John Naylor from Ground-Gas Solutions for providing data from their survey of the landfill site. We would like to thank David Hodgetts from the School of Earth and Environmental Sciences, The University of Manchester, for providing the lidar survey data. From the School of Chemistry at the University of Bristol, we would like to thank James C. Matthews, Matthew D. Wright, Damien Martin and Dudley Shallcross for conducting the tracer release experiment. Many thanks to Thorsten Warneke and Hella van Asperen from the Institute of Environmental Physics (IUP), University of Bremen, for their advise on the deployment of the FTIR. We also thank Peter Somkuti for processing the meteorological data. This research used the ALICE High Performance Computing facility at the University of Leicester.

Edited by: Christof Ammann
Reviewed by: Werner Eugster and one anonymous referee

References

Allen, G., Gallagher, M., Hollingsworth, P., Illingworth, S., Kabbabe, K., and Percival, C.: Feasibility of aerial measurements of methane emissions from landfills, Environment Agency, Bristol, UK, 2014.

Allen, G., Pitt, J., Hollingsworth, P., Mead, I., Kabbabe, K., Roberts, G., and Percival, C.: Measuring landfill methane emissions using unmanned aerial systems: field trial and operational guidance, Environment Agency, Bristol, UK, 2015.

Baer, D., Paul, J., Gupta, M., and O'Keefe, A.: Sensitive absorption measurements in the near-infrared region using off-axis integrated-cavity-output spectroscopy, Appl. Phys. B, 75, 261–265, 2002.

Bell, M., Flechard, C., Fauvel, Y., Häni, C., Sintermann, J., Jocher, M., Menzi, H., Hensen, A., and Neftel, A.: Ammonia emissions from a grazed field estimated by miniDOAS measurements and inverse dispersion modelling, Atmos. Meas. Tech., 10, 1875–1892, https://doi.org/10.5194/amt-10-1875-2017, 2017.

Bergamaschi, P., Lubina, C., Königstedt, R., Fischer, H., Veltkamp, A. C., and Zwaagstra, O.: Stable isotopic signatures ($\delta^{13}C$, δD) of methane from European landfill sites, J. Geophys. Res.-Atmos., 103, 8251–8265, 1998.

Bogner, J., Spokas, K., Burton, E., Sweeney, R., and Corona, V.: Landfills as atmospheric methane sources and sinks, Chemosphere, 31, 4119–4130, 1995.

Börjesson, G., Danielsson, Å., and Svensson, B. H.: Methane fluxes from a Swedish landfill determined by geostatistical treatment of static chamber measurements, Environ. Sci. Technol., 34, 4044–4050, 2000.

Brown, P., Broomfield, M., Buys, G., Cardenas, L., Kilroy, E., MacCarthy, J., Murrells, T., Pang, Y., Passant, N., Ramirez Garcia, J., Thistlethwaite, G., and Webb, N.: UK greenhouse gas inventory, 1990 to 2014: annual report for submission under the Framework Convention on Climate Change, Ricardo Energy & Environment, Harwell, Didcot, UK, 2016.

Buccolieri, R. and Sabatino, S. D.: MUST experiment simulations using CFD and integral models, Int. J. Environ. Poll., 44, 376–384, 2011.

Christophersen, M., Kjeldsen, P., Holst, H., and Chanton, J.: Lateral gas transport in soil adjacent to an old landfill: factors governing emissions and methane oxidation, Waste Manage. Res., 19, 595–612, 2001.

Czepiel, P. M., Mosher, B., Harriss, R. C., Shorter, J. H., McManus, J. B., Kolb, C. E., Allwine, E., and Lamb, B. K: Landfill methane emissions measured by enclosure and atmospheric tracer methods, J. Geophys. Res.-Atmos., 101, 16711–16719, 1996.

Delkash, M., Zhou, B., Han, B., Chow, F. K., Rella, C. W., and Imhoff, P. T.: Short-term landfill methane emissions dependency on wind, Waste Manage., 55, 288–298, 2016.

Di Trapani, D., Di Bella, G., and Viviani, G.: Uncontrolled methane emissions from a MSW landfill surface: Influence of landfill features and side slopes, Waste Manage., 33, 2108–2115, 2013.

Dlugokencky, E. J., Nisbet, E. G., Fisher, R., and Lowry, D.: Global atmospheric methane: budget, changes and dangers, Philos. T. Roy. Soc. Lond. A, 369, 2058–2072, 2011.

Flesch, T. K., Wilson, J. D., and Yee, E.: Backward-time Lagrangian stochastic dispersion models and their application to estimate gaseous emissions, J. Appl. Meteorol., 34, 1320–1332, 1995.

Flesch, T. K., Wilson, J., Harper, L., Crenna, B., and Sharpe, R.: Deducing ground-to-air emissions from observed trace gas concentrations: a field trial, J. Appl. Meteorol., 43, 487–502, 2004.

Flesch, T. K., Harper, L. A., Desjardins, R. L., Gao, Z., and Crenna, B. P.: Multi-source emission determination using an inverse-dispersion technique, Boundary-Lay. Meteorol., 132, 11–30, 2009.

Foster-Wittig, T. A., Thoma, E. D., Green, R. B., Hater, G. R., Swan, N. D., and Chanton, J. P.: Development of a mobile tracer correlation method for assessment of air emissions from landfills and other area sources, Atmos. Environ., 102, 323–330, 2015.

Galle, B., Samuelsson, J., Svensson, B. H., and Börjesson, G.: Measurements of methane emissions from landfills using a time correlation tracer method based on FTIR absorption spectroscopy, Environ. Sci. Technol., 35, 21–25, 2001.

Gebert, J., Röwer, I. U., Scharff, H., Roncato, C. D., and Cabral, A. R.: Can soil gas profiles be used to assess microbial CH_4 oxidation in landfill covers?, Waste Manage., 31, 987–994, 2011.

Gonzalez-Valencia, R., Magana-Rodriguez, F., Cristóbal, J., and Thalasso, F.: Hotspot detection and spatial distribution of methane emissions from landfills by a surface probe method, Waste Manage., 55, 299–305, 2016.

Griffith, D. W. T., Deutscher, N. M., Caldow, C., Kettlewell, G., Riggenbach, M., and Hammer, S.: A Fourier transform infrared trace gas and isotope analyser for atmospheric applications, Atmos. Meas. Tech., 5, 2481–2498, https://doi.org/10.5194/amt-5-2481-2012, 2012.

Hammer, S., Griffith, D. W. T., Konrad, G., Vardag, S., Caldow, C., and Levin, I.: Assessment of a multi-species in situ FTIR for precise atmospheric greenhouse gas observations, Atmos. Meas. Tech., 6, 1153–1170, https://doi.org/10.5194/amt-6-1153-2013, 2013.

Hargreaves, D. and Wright, N. G.: On the use of the k–ε model in commercial CFD software to model the neutral atmospheric boundary layer, J. Wind Eng. Indust. Aerodynam., 95, 355–369, 2007.

Hodgetts, D.: Laser scanning and digital outcrop geology in the petroleum industry: a review, Mar. Petrol. Geol., 46, 335–354, 2013.

Hrad, M., Binner, E., Piringer, M., and Huber-Humer, M.: Quantification of methane emissions from full-scale open windrow composting of biowaste using an inverse dispersion technique, Waste Manage., 34, 2445–2453, 2014.

Jeanjean, A. P. R.: Modelling the Impact of Trees on Vehicular Emissions in the Urban Environment Using Computational Fluid Dynamics, PhD thesis, Department of Physics and Astronomy, University of Leicester, Leicester, UK, http://hdl.handle.net/2381/39572, last access: 10 September 2017.

Jeanjean, A. P. R., Hinchliffe, G., McMullan, W., Monks, P. S., and Leigh, R. J.: A CFD study on the effectiveness of trees to disperse road traffic emissions at a city scale, Atmos. Environ., 120, 1–14, 2015.

Jeanjean, A. P. R., Buccolieri, R., Eddy, J., Monks, P. S., and Leigh, R.: Air quality affected by trees in real street canyons: The case of Marylebone neighbourhood in central London, Urb. Forest. Urb. Green., 22, 41–53, 2017.

Launder, B. E., Reece Jr., G., and Rodi, W.: Progress in the development of a Reynolds-stress turbulence closure, J. Fluid. Mech., 68, 537–566, 1975.

Leelőssy, Á., Molnár, F., Izsák, F., Havasi, Á., Lagzi, I., and Mészáros, R.: Dispersion modeling of air pollutants in the atmosphere: a review, Centr. Eur. J. Geosci., 6, 257–278, https://doi.org/10.2478/s13533-012-0188-6, 2014.

Lefer, B. L., Talbot, R. W., Harriss, R. H., Bradshaw, J. D., Sandholm, S. T., Olson, J. O., Sachse, G. W., Collins, J., Shipham, M. A., Blake, D. R., Klemm, K. I., Klemm, O., Gorzelska, K., and Barrick, J.: Enhancement of acidic gases in biomass burning impacted air masses over Canada, J. Geophys. Res.-Atmos., 99, 1721–1737, 1994.

legislation.gov.uk: Climate Change Act 2008, available at: http://www.legislation.gov.uk/ukpga/2008/27/section/1, last access: 20 June 2017.

Lohila, A., Laurila, T., Tuovinen, J.-P., Aurela, M., Hatakka, J., Thum, T., Pihlatie, M., Rinne, J., and Vesala, T.: Micrometeorological measurements of methane and carbon dioxide fluxes at a municipal landfill, Environ. Sci. Technol., 41, 2717–2722, 2007.

Mazzoldi, A., Hill, T., and Colls, J. J.: CFD and Gaussian atmospheric dispersion models: A comparison for leak from carbon dioxide transportation and storage facilities, Atmos. Environ., 42, 8046–8054, 2008.

Mønster, J. and Scheutz, C.: Quantification of the methane emission from Masons landfill – Part II, Tech. Rep., Department of Environmental Engineering, Technical University of Denmark (DTU), Kgs. Lyngby, Denmark, 2015.

Mønster, J., Samuelsson, J., Kjeldsen, P., and Scheutz, C.: Quantification of methane emissions from 15 Danish landfills using the mobile tracer dispersion method, Waste Manage., 35, 177–186, 2015.

Mønster, J. G., Samuelsson, J., Kjeldsen, P., Rella, C. W., and Scheutz, C.: Quantifying methane emission from fugitive sources by combining tracer release and downwind measurements – a sensitivity analysis based on multiple field surveys, Waste Manage., 34, 1416–1428, 2014.

Myhre, G., Shindell, D., Bréon, F.-M., Collins, W., Fuglestvedt, J., Huang, J., Koch, D., Lamarque, J.-F., Lee, D., Mendoza, B., Nakajima, T., Robock, A., Stephens, G., Takemura, T., and Zhang, H.: Anthropogenic and natural radiative forcing, in: Climate Change 2013: The physical science basis, Climate Change, 423, 659–740, 2013.

Parra, M. A., Santiago, J. L., Martin, F., Martilli, A., and Santamaria, J. M.: A methodology to urban air quality assessment during large time periods of winter using computational fluid dynamic models, Atmos. Environ., 44, 2089–2097, 2010.

Pratt, C., Walcroft, A. S., Deslippe, J., and Tate, K. R.: CH_4/CO_2 ratios indicate highly efficient methane oxidation by a pumice landfill cover-soil, Waste Manage., 33, 412–419, 2013.

Rachor, I. M., Gebert, J., Gröngröft, A., and Pfeiffer, E.-M.: Variability of methane emissions from an old landfill over different time-scales, Eur. J. Soil Sci., 64, 16–26, 2013.

Riddick, S., Hancock, B., Robinson, A. D., Connors, S., Davies, S., Allen, G., and Pitt, J.: Development of a low-maintenance measurement approach to continuously estimate methane emissions: a case study, Waste Manage., in press, 2016.

Riddle, A., Carruthers, D., Sharpe, A., McHugh, C., and Stocker, J.: Comparisons between FLUENT and ADMS for atmospheric dispersion modelling, Atmos. Environ., 38, 1029–1038, 2004.

Rinne, J., Pihlatie, M., Lohila, A., Thum, T., Aurela, M., Tuovinen, J.-P., Laurila, T., and Vesala, T.: Nitrous oxide emissions from a municipal landfill, Environ. Sci. Technol., 39, 7790–7793, 2005.

Salisbury, E., Hampshire, K., Brook, R., Buys, G., Bailey, R., Thistlethwaite, G., Walker, C., Wakeling, D., Brown, P., Pang, Y., and Cardenas, L.: Greenhouse Gas Inventories for England, Scotland, Wales and Northern Ireland: 1990–2014, Aether, Oxford, UK, 2016.

Santiago, J., Borge, R., Martin, F., de la Paz, D., Martilli, A., Lumbreras, J., and Sanchez, B.: Evaluation of a CFD-based approach to estimate pollutant distribution within a real urban canopy by means of passive samplers, Sci. Total Environ., 576, 46–58, 2017.

Scheutz, C., Kjeldsen, P., Bogner, J. E., De Visscher, A., Gebert, J., Hilger, H. A., Huber-Humer, M., and Spokas, K.: Microbial methane oxidation processes and technologies for mitigation of landfill gas emissions, Waste Manage. Res., 27, 409–455, 2009.

Scheutz, C., Samuelsson, J., Fredenslund, A. M., and Kjeldsen, P.: Quantification of multiple methane emission sources at landfills using a double tracer technique, Waste Manage., 31, 1009–1017, 2011.

Schroth, M. H., Eugster, W., Gómez, K. E., Gonzalez-Gil, G., Niklaus, P. A., and Oester, P: Above-and below-ground methane fluxes and methanotrophic activity in a landfill-cover soil, Waste Manage., 32, 879–889, 2012.

Themelis, N. J. and Ulloa, P. A.: Methane generation in landfills, Renewable Energy, 32, 1243–1257, 2007.

Tominaga, Y. and Stathopoulos, T.: Turbulent Schmidt numbers for CFD analysis with various types of flowfield, Atmos. Environ., 41, 8091–8099, 2007.

WMO: Guide to Meteorological Instruments and Methods of Observation, Report, Geneva, Switzerland, 2008.

Yokelson, R. J., Andreae, M. O., and Akagi, S. K.: Pitfalls with the use of enhancement ratios or normalized excess mixing ratios measured in plumes to characterize pollution sources and aging, Atmos. Meas. Tech., 6, 2155–2158, https://doi.org/10.5194/amt-6-2155-2013, 2013.

Yver Kwok, C. E., Müller, D., Caldow, C., Lebègue, B., Mønster, J. G., Rella, C. W., Scheutz, C., Schmidt, M., Ramonet, M., Warneke, T., Broquet, G., and Ciais, P.: Methane emission estimates using chamber and tracer release experiments for a municipal waste water treatment plant, Atmos. Meas. Tech., 8, 2853–2867, https://doi.org/10.5194/amt-8-2853-2015, 2015.

Zhu, H., Letzel, M. O., Reiser, M., Kranert, M., Bächlin, W., and Flassak, T.: A new approach to estimation of methane emission rates from landfills, Waste Manage., 33, 2713–2719, 2013.